SPATIOTEMPORAL VARIATION OF GASEOUS POLLUTANTS AND PARTICULATE MATTER AT GRANITE QUARRY SITES IN ABUJA, NIGERIA

George, C.[1], Tukura, B.W.[1], Opaluwa, O.D.[1] and Ngasoh, F.G.[2*]

[1]Department of Chemistry, Faculty of Natural and Applied Sciences, Nasarawa State University, Keffi, Nasarawa State, Nigeria

[2]Department of Agricultural and Bioresources Engineering, Taraba State University, Jalingo, Nigeria

[*]Corresponding email: felixngasoh@gmail.com

ABSTRACT

Granite quarrying supplies aggregate for the rapid growth of Abuja, but its emissions to air have rarely been characterised in space and time. Carbon monoxide (CO), nitrogen dioxide (NO_2), sulphur dioxide (SO_2), $PM_{2.5}$ and PM_{10} were monitored with portable analysers at 22 sampling points in three active quarries at Dutse and Mpape, Federal Capital Territory, at 08:00, 12:00 and 17:00 h from January to June 2025 (396 observations per pollutant). $PM_{2.5}$ (median 37.3 µg/m³) exceeded the WHO 24-h guideline in 98% of observations, and PM_{10} exceeded its guideline in every January–February observation but in only 6% in May–June. Month explained 15–50% of the variance in log concentrations, sampling point 15–35% and time of day ≤ 8%. From the harmattan to the wet season, mean PM_{10}, $PM_{2.5}$, CO and NO_2 fell by 57–84%. Diesel power houses had higher CO and SO_2 than the other work points at all quarries and higher NO_2 at the two Dutse quarries, whereas PM did not differ. Hierarchical clustering and principal component analysis separated a general background from three hotspot types: power houses (combustion), a haul road with episodic $PM_{2.5}$ above 800 µg/m³ (dust) and a market with high CO (mean 25.5 ppm). No observation was rated "Good" on the air quality index, and 65% of harmattan observations were "Unhealthy" or worse. $PM_{2.5}/PM_{10}$ ratios above 1 in 94% of wet-season records indicate humidity bias in the optical sensor, and the 0.1 ppm resolution of the NO_2 and SO_2 sensors limits comparison with guidelines. Haul-road dust suppression, cleaner power supply, seasonal controls and reference-grade monitoring are recommended.

Keywords: Quarry dust; particulate matter; spatial distribution; air quality index; harmattan; diesel generators; low-cost sensors; Abuja; Nigeria

1 INTRODUCTION

Rapid urban growth in Nigeria's Federal Capital Territory (FCT) has created a strong demand for crushed granite aggregate, and many quarries operate on the inselbergs and ridges that border built-up districts. Drilling, blasting, crushing, screening, loading and haulage release particulate matter (PM) directly into the air. The diesel generators, crushers and trucks that power these operations emit carbon monoxide (CO), nitrogen oxides and sulphur dioxide (SO_2). Fine particles ($PM_{2.5}$) penetrate deep into the lungs and are associated with cardiopulmonary disease and premature mortality, while coarse dust, including crystalline-silica-bearing granite dust, affects the airways and contributes to occupational lung disease [1, 2]. Workers in quarries are therefore exposed both to

mechanically generated dust and to combustion products, and people working or trading near the quarries may share part of that exposure. Studies of quarry air quality in Nigeria have reported particulate concentrations above national and international limits near quarries in Cross River State [3], in the Mpape area of Abuja [4] and at granite processing sites elsewhere in Abuja [5], and mining has long been recognised as a major source of fugitive PM [6]. Most such studies, however, report concentrations at a few points over a short campaign, or compare sites without resolving how pollution varies between individual activity areas within a quarry, between seasons and across the working day. In the Guinea savanna of central Nigeria, the year moves from the dusty harmattan, when north-easterly winds carry Saharan and Sahelian dust southward [7], to humid monsoon months, when rainfall suppresses re-suspension and removes particles from the air. Diurnal changes in boundary-layer mixing and work intensity add further variation [8]. Without separating these influences, it is difficult to identify the dominant sources within a quarry, to decide when controls are most needed, or to interpret single-visit measurements. This study examined five pollutants (CO, NO_2, SO_2, $PM_{2.5}$ and PM_{10}) at 22 sampling points in three active granite quarries in Dutse and Mpape, FCT, over six months spanning the harmattan, transition and early wet season, at three times of day. The objectives were to (i) quantify concentrations and their exceedance of WHO [1] guidelines; (ii) partition the variability among sampling points, months and times of day; (iii) map and characterise the spatial distribution of pollutants within each quarry and identify hotspot types using multivariate analysis; and (iv) classify air quality with the air quality index (AQI) and evaluate the reliability of the portable-sensor data.

2. MATERIALS AND METHODS

2.1 Study area

The study was conducted at three commercial granite quarries in Bwari Area Council, FCT (Figure 1). Two quarries (Q1 and Q2) are on the Dutse hills, and the third (Q3) is on the Mpape ridge to the east, beside the densely populated Mpape settlement [4]. The rocks are Precambrian Basement Complex granites, migmatites and gneisses. The climate is tropical wet-and-dry, with a harmattan-influenced dry season from about November to March and a rainy season from about April to October.

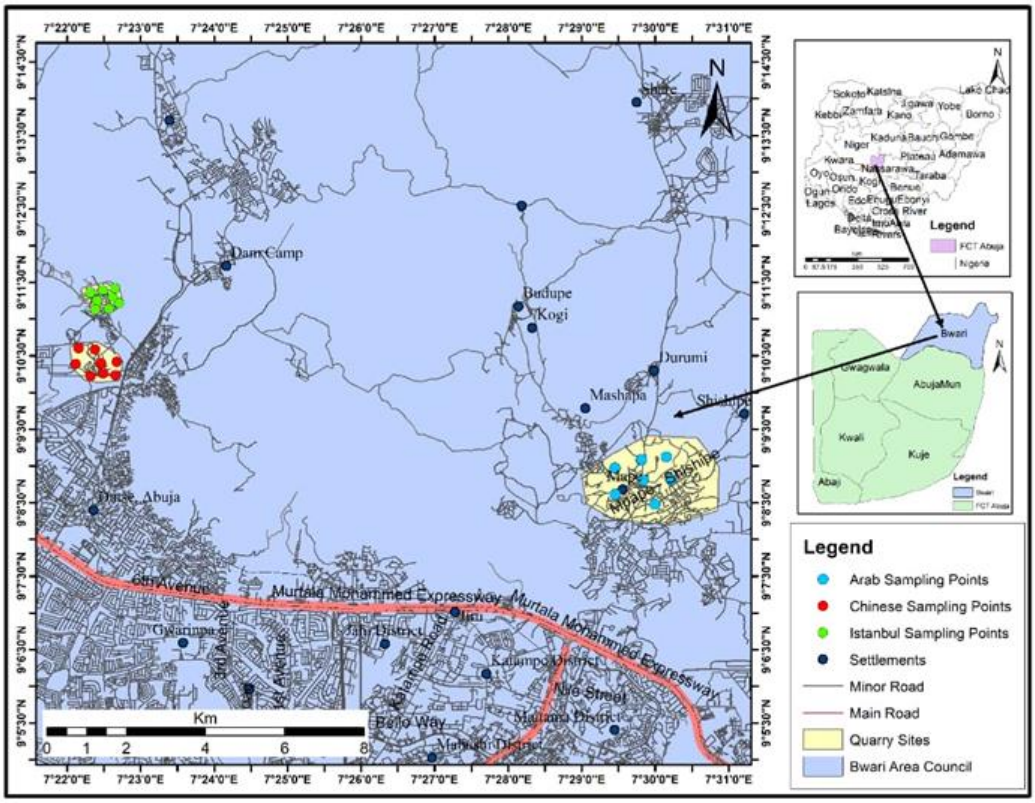

Figure 1. Location of the three quarries and sampling points in Bwari Area Council, FCT, Abuja. Red: Q1 (Dutse); green: Q2 (Dutse); blue: Q3 (Mpape)

2.2 Sampling points

Eight sampling points were monitored at Q1 and Q2 and six at Q3, giving 22 in total. Sampling points were selected following the general principles for planning ambient air sampling in ASTM D1357 [9], so that they represented the main emission sources (power houses and haul roads), the general working area, the site boundary (quarry gate) and nearby receptor locations (market, school and outside the quarry). The points are identified by the labels used in the field (Table 1). At each quarry they comprised one or two general work points (Point 1, Point 2), the two diesel power houses that supply the crushers (Power house 1 and 2), the quarry gate, and a point recorded as "Outside quarry". Q1 also included two named locations, a market and Noble School; Q2 included two haul roads (Zone A Road 1 and Road 2); and Q3 included a market. The Q2 haul road recorded as "Zone A Road 2" in January, May and June and "Zone B Road 2" in February–April is treated here as a single point, Zone A/B Road 2. The coordinates of each point were recorded by GPS and used for the spatial interpolation (Section 2.5).

Table 1. Sampling points monitored at each quarry (labels as recorded in the field)

Quarry	Sampling points	n
Q1 (Dutse)	Point 1; Point 2; Power house 1; Power house 2; Quarry gate; Outside quarry; Market; Noble School	8
Q2 (Dutse)	Point 1; Point 2; Power house 1; Power house 2; Quarry gate; Outside quarry; Zone A Road 1; Zone A/B Road 2	8
Q3 (Mpape)	Point 1; Power house 1; Power house 2; Quarry gate; Outside quarry; Market	6

2.3 Measurements

CO, NO_2, SO_2, $PM_{2.5}$ and PM_{10} were measured with portable air-quality monitors fitted with electrochemical gas sensors (CO, NO_2 and SO_2) and an optical particle sensor ($PM_{2.5}$ and PM_{10}) using Aeroqual series 500. Judged from the recorded values, the effective resolution of the NO_2 and SO_2 sensors was about 0.1 ppm (Section 3.1). No field calibration against reference or gravimetric instruments was carried out during the campaign; the consequences for data quality are assessed in Sections 2.7 and 3.8. Measurements were made at about 1.5 m above ground (breathing-zone height) [9], three times a week from January to June 2025, in three daily rounds in the morning (around 08:00), afternoon (around 12:00) and evening (around 17:00). Within each round the sampling points were visited in sequence, so the stated times identify rounds centred on those hours rather than simultaneous measurements. At each visit the instrument was allowed to stabilise before the reading was recorded. Readings were averaged by sampling point, time of day and month, giving 22 points × 6 months × 3 times = 396 observations per pollutant; each observation is therefore a monthly mean for one point and time of day. Gases are reported in ppm and PM in µg/m³; conversions between ppm and µg/m³ assume 25 °C and 1 atm [10]. Months were grouped into the harmattan (January–February), transition (March–April) and wet season (May–June). The data set forms part of a wider study of air pollutants and heavy metals at quarry sites in the FCT [11].

2.4 Guidelines and air quality index

PM was compared with the WHO [1] 24-h guidelines ($PM_{2.5}$ 15 µg/m³; PM_{10} 45 µg/m³). Because each reading was a short spot measurement, gases were compared both with the WHO short-term guidelines (NO_2 1-h 200 µg/m³ ≈ 0.106 ppm; SO_2 10-min 500 µg/m³ ≈ 0.191 ppm; CO 1-h 35 mg/m³ ≈ 30.5 ppm and 8-h 10 mg/m³ ≈ 8.7 ppm) and with the 24-h guidelines (NO_2 25 µg/m³ ≈ 0.013 ppm; SO_2 40 µg/m³ ≈ 0.015 ppm; CO 4 mg/m³ ≈ 3.5 ppm). Spot and averaged readings are not equivalent to the guideline averaging periods, so exceedances are indicative. An air quality index (AQI) sub-index was calculated for each observation of $PM_{2.5}$, PM_{10} and CO by linear interpolation between the U.S. EPA [12] breakpoints (Eq. 1).

$$I_p = \frac{I_{Hi} - I_{Lo}}{BP_{Hi} - BP_{Lo}}\left(C_p - BP_{Lo}\right) + I_{Lo} \quad (1)$$

where C_p is the concentration of pollutant p (truncated to one decimal place for $PM_{2.5}$ and CO and to an integer for PM_{10}), BP_{Hi} and BP_{Lo} are the breakpoints that bracket C_p, and I_{Hi} and I_{Lo} are the index values for those breakpoints. The overall index was expressed as in Eq. 2.

$$AQI = max(I_{PM2.5}, I_{PM10}, I_{CO}) \quad (2)$$

The AQI categories are Good (0–50), Moderate (51–100), Unhealthy for Sensitive Groups [USG] (101–150), Unhealthy (151–200), Very Unhealthy (201–300) and Hazardous (> 300); the category and the dominant pollutant were recorded for each observation. NO_2 and SO_2 were excluded from the AQI because their breakpoints lie near the sensor resolution. Because the EPA breakpoints are defined for 24-h PM and 8-h CO averages, AQI values calculated here from short-term readings indicate the category of air quality but are not formal AQI reports.

2.5 Spatial interpolation and statistical analysis

The spatial distribution of each pollutant within each quarry was mapped by interpolating the six-month mean concentration at each sampling point onto a regular grid and contouring using inverse distance weighting (IDW) [13] in Surfer version 28. Concentrations were $\log_{10}$-transformed (offsets 0.01 ppm for gases and 1 µg/m³ for PM). The variance of each pollutant was partitioned with a three-factor main-effects linear model containing sampling point (22 levels, which include site differences), month (6 levels) and time of day (3 levels). The unique sum of squares of each factor (type II) was expressed as a percentage of the total, with F-tests for significance [14]. Because the design is balanced, these percentages and the residual sum to about 100%. Differences between quarries were tested with the Kruskal–Wallis test [15]. Power houses were compared with the other work points (Points 1–2) at the same site, month and time with the Wilcoxon signed-rank test [16]. Time-of-day effects were confirmed with the paired Friedman test [17] (blocks: point-months). Spearman correlation [18] and principal component analysis (PCA) [19] of standardised log concentrations (Eq.3) were used to identify co-varying pollutants.

$$z_{ip} = \frac{y_{ip} - \bar{y}_p}{s_p}, \; Rv_m = \lambda_m v_m, \; a_{pm} = v_{pm}\sqrt{\lambda_m}, \; t_{im} = \sum_p z_{ip}\, v_{pm} \quad (3)$$

where z_{ip} is the standardised value of pollutant p in observation i, R the correlation matrix, λ_m and v_m the m-th eigenvalue and eigenvector, a_{pm} the loading of pollutant p on component m, and t_{im} the component score. The variance explained by component m is 100 λ_m / Σ λ. Sampling points were grouped objectively by Ward's hierarchical clustering of their standardised mean log profiles, which merges at each step the two clusters A and B that minimise the increase in within-cluster sum of squares [20].

$$\Delta(A,B) = \left[\frac{n_A n_B}{n_A + n_B}\right] \|c_A - c_B\|^2 \quad (4)$$

where n_A and n_B are the numbers of points in each cluster and c_A and c_B their centroids. Analyses were performed in Python (pandas, NumPy, SciPy), with significance at $p < 0.05$. Because the 18 observations at each sampling point are repeated measurements of the same location, they are not fully independent, and p-values from tests that treat them as independent are likely to be too small. The comparisons between quarries and between power houses and other work points were therefore repeated on the 22 six-month point means (Kruskal–Wallis and Mann–Whitney tests) [15, 21], treating each sampling point as one independent unit.

2.6 Indicative health-risk estimates

To express the health significance of $PM_{2.5}$, the excess short-term risk of all-cause mortality relative to the WHO 24-h guideline was estimated with the log-linear concentration–response function of Orellano et al. [22] using Eq. 5.

$$\Delta R(\%) = 100 \times \left[\frac{R_{R10}(C - C_{\text{ref}})}{10} - 1\right] \quad (5)$$

Where R_{R10} = 1.0065 is the relative risk per 10 µg/m³ increase in daily $PM_{2.5}$, C the mean concentration for the period considered and C_{ref} = 15 µg/m³. For long-term exposure, the relative risk compared with the WHO annual guideline was estimated from the meta-analysis of Chen and Hoek [23] (Eq 6).

$$RR = \frac{RR10(C-5)}{10} \quad (6)$$

with RR_{10} = 1.08 per 10 µg/m³. The fraction of all-cause mortality among exposed people attributable to $PM_{2.5}$ above the guideline was then expressed as Eq. 7 [24].

$$AF = \frac{(RR-1)}{RR} \quad (7)$$

These estimates are illustrative because the measurements are daytime spot readings over six months rather than personal, year-round exposures.

2.7 Sensor data-quality check

Because $PM_{2.5}$ is a size fraction of PM_{10}, the ratio $r_{PM} = PM_{2.5}/PM_{10}$ cannot physically exceed 1. The ratio was calculated for every observation and used as an internal check on the optical particle sensor; values above 1 indicate measurement bias.

3 RESULTS AND DISCUSSION

3.1 Concentrations, guideline exceedance and comparison with other studies

Summary statistics are given in Table 2. $PM_{2.5}$ ranged from 10.5 to 816 µg/m³ (mean 55.5 µg/m³; median 37.3 µg/m³) and PM_{10} from 6.6 to 904 µg/m³ (mean 63.0 µg/m³; median 34.0 µg/m³). Both distributions were strongly right-skewed because of one haul road at Q2 (Section 3.4). The median $PM_{2.5}$ was 2.5 times the WHO 24-h guideline, and 98% of observations exceeded it, including 94% in the wet season. PM_{10} exceeded 45 µg/m³ in 40% of observations overall, but this proportion fell from 100% in the harmattan to 14% in the transition period and 6% in the wet season. The quarries differed significantly in CO, NO_2, $PM_{2.5}$ and PM_{10} (Kruskal–Wallis, $p \leq 0.012$) but not in SO_2 (p = 0.87). When this comparison was repeated on the 22-point means (n = 8, 8 and 6), which avoids treating repeated observations at a point as independent, only NO_2 differed significantly between quarries (Kruskal–Wallis p = 0.038); $PM_{2.5}$ was marginal (p = 0.062), and CO, SO_2 and PM_{10} did not differ (p = 0.13–0.93). Differences between quarries should therefore be interpreted with caution.

Table 2. Concentrations at the three quarries, January–June 2025: mean ± SD (first line) and median (range) (second line). n = 144 (Q1), 144 (Q2), 108 (Q3) and 396 (all sites)

Pollutant	Q1 (Dutse)	Q2 (Dutse)	Q3 (Mpape)	All sites
CO (ppm)	1.39 ± 1.87 0.40 (0.00–6.50)	1.68 ± 1.73 1.10 (0.00–6.40)	5.80 ± 9.35 1.60 (0.00–36.00)	2.70 ± 5.45 1.00 (0.00–36.00)
NO_2 (ppm)	0.205 ± 0.373 0.100 (0.000–2.010)	0.222 ± 0.364 0.100 (0.000–2.200)	0.091 ± 0.064 0.100 (0.000–0.200)	0.180 ± 0.320 0.100 (0.000–2.200)
SO_2 (ppm)	0.059 ± 0.065 0.030 (0.000–0.300)	0.068 ± 0.091 0.035 (0.000–0.500)	0.062 ± 0.055 0.100 (0.000–0.200)	0.063 ± 0.073 0.080 (0.000–0.500)
$PM_{2.5}$ (µg/m³)	39.3 ± 22.1 27.0 (10.5–86.0)	73.3 ± 156.7 35.0 (17.0–816.0)	53.6 ± 26.5 46.1 (20.0–151.0)	55.5 ± 97.3 37.2 (10.5–816.0)
PM_{10} (µg/m³)	47.0 ± 39.5 23.0 (6.6–141.0)	84.6 ± 175.8 30.0 (13.0–904.0)	55.5 ± 30.1 43.8 (18.0–162.0)	63.0 ± 110.8 34.0 (6.6–904.0)

Excluding Zone A/B Road 2 in March–April, Q2 means are 41.1 µg/m³ ($PM_{2.5}$) and 49.2 µg/m³ (PM_{10}).

CO averaged 2.70 ppm (median 1.00 ppm), with the highest site mean at Q3 (5.80 ppm) because of its market sampling point. CO exceeded the WHO 24-h guideline (approximately 3.5 ppm) in 23% of observations and the 8-h guideline (approximately 8.7 ppm) in 4.5%. It exceeded the 1-h guideline (≈ 30.5 ppm) in 1% of observations, all at the Q3 market in January–February. NO_2 (mean 0.18 ppm)

exceeded the 1-h guideline (approximately 0.106 ppm) in 32% of observations, mostly in the harmattan and at the power houses. SO_2 (mean 0.063 ppm) exceeded the 10-min guideline in 7%. Because the effective sensor resolution is about 0.1 ppm (see below), these NO_2 and SO_2 exceedances correspond in practice to readings of 0.2 ppm or more and are indicative only. However, even after averaging, 83% of NO_2 and 90% of SO_2 values fell on a 0.1 ppm grid, and 17% and 41% respectively were zero. This indicates an effective sensor resolution of about 0.1 ppm, roughly seven times the WHO 24-h guidelines, so compliance with those guidelines cannot be judged and the gas data are best used for relative comparisons. The $PM_{2.5}$ levels around the Abuja quarries (median 37 µg/m³; harmattan mean 67 µg/m³) are well above the annual means of 17–26 µg/m³ measured with calibrated sensors at urban sites in Abidjan and Accra [25]. They lie within the range reported for other Nigerian quarries. The closest comparison is the study of Ayegba et al. [5] at two granite quarries elsewhere in Abuja (Pyakassa and Daijinja), with which our results agree in three respects. Both studies found $PM_{2.5}$ above the 24-h limits at all monitored locations. Both found higher concentrations in the dry than in the rainy season. And both found the combustion gas CO to be distributed differently from PM, being linked to vehicle and equipment locations rather than the crushing area. Their measured dry-season $PM_{2.5}$ at processing points (27–30 µg/m³ over short sampling intervals) is lower than ours, but their estimated 24-h equivalents (160–180 µg/m³) are higher. This shows how strongly reported values depend on sampling duration and averaging conventions, which should be stated explicitly when quarry studies are compared. Much higher levels have been reported at a quarry in Akamkpa, Cross River State, where $PM_{2.5}$ ranged from 127 to 292 µg/m³ in the dry season and 92 to 240 µg/m³ in the wet season [3]. Our values sit at the lower to middle end of this range, except for the Q2 haul road, whose March–April peaks (above 800 µg/m³) exceed all of them. Earlier work in the Mpape area also reported particulate and gaseous pollution around quarries above Nigerian limits [4], consistent with the elevated levels we found at Q3.

3.2 Sources of variability

Table 3 partitions the variance of each pollutant among sampling point, month and time of day, using the type II sums of squares of the main-effects model [14]. Month was the largest factor for CO (48%), NO_2 (28%) and PM_{10} (50%), and was about equal to sampling point for SO_2 (15% and 16%). For $PM_{2.5}$, sampling point explained more variance (35%) than month (30%), largely because of the haul road at Q2. A similar dominance of season over site has been reported in multi-year fine-particle records from six sites in Akure, south-western Nigeria [26]. Time of day explained 8% of the variance for SO_2, 3% for NO_2, under 1% for CO and nothing for PM ($p > 0.85$). Residual variance, which includes interactions such as hotspots that appear only in some months, was 25–35% for CO and PM but 54–61% for NO_2 and SO_2. The high residuals for these two gases are consistent with their coarse sensor resolution [27, 28].

Table 3. Variance partitioning of log-transformed concentrations: % of total sum of squares (F; p)

Pollutant	Sampling point (df = 21)	Month (df = 5)	Time of day (df = 2)	Residual % (df = 367)
CO	26.3 (18.2; <0.001)	47.8 (139.1; <0.001)	0.7 (5.1; 0.007)	25.2
NO_2	14.9 (4.9; <0.001)	27.9 (38.0; <0.001)	3.4 (11.7; <0.001)	53.8
SO_2	15.8 (4.6; <0.001)	15.1 (18.3; <0.001)	8.4 (25.6; <0.001)	60.6
$PM_{2.5}$	35.3 (17.8; <0.001)	30.1 (63.9; <0.001)	0.0 (0.1; 0.891)	34.6
PM_{10}	21.1 (12.8; <0.001)	50.1 (127.5; <0.001)	0.0 (0.2; 0.858)	28.8

3.3 Seasonal and diurnal variation

All pollutants peaked in January–February and declined sharply into the wet season (Figure 2). Between the harmattan and the wet season, mean PM_{10} fell from 93.5 to 25.5 µg/m³ (−73%), $PM_{2.5}$ from 67.2 to 29.1 µg/m³ (−57%), CO from 5.19 to 1.22 ppm (−76%), NO_2 from 0.38 to 0.06 ppm (−84%) and SO_2 from 0.098 to 0.030 ppm (−69%). The decline was steepest between February and March for PM and CO at Q1 and Q3, whereas NO_2 at the Dutse quarries fell mainly within or at the end of the harmattan (Q1, January to February; Q2, February to March) and changed little at Q3. Q2 departed

from this pattern in March–April because of its haul road, and Q3 kept higher CO throughout because of its market point. Comparable harmattan maxima and wet-season minima have been reported for fine particles in Akure (dry-season mean about 77 µg/m³ against about 20 µg/m³ in the wet season) [26] and Ibadan [29], and at two granite quarries elsewhere in Abuja [5].

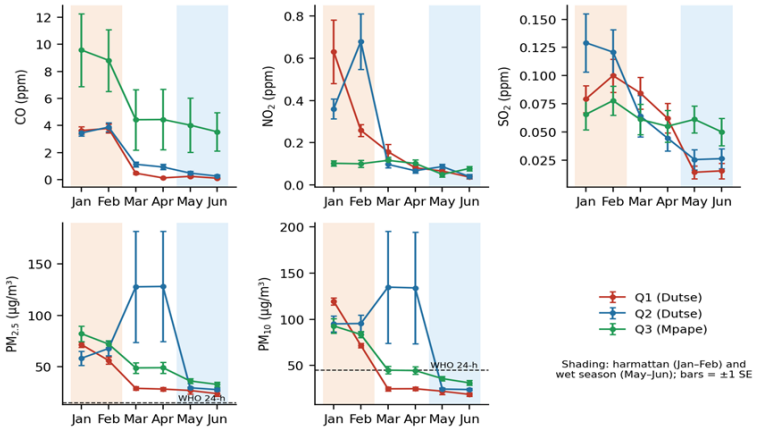

Figure 2. Monthly mean concentrations (± 1 SE) at the three quarries. Shading marks the harmattan (January–February) and the wet season (May–June); dashed lines are WHO [1] 24-h guidelines

Seasonal timing explained more of the variance than location for most pollutants (Table 3). This is attributed to three processes acting together. The first is the regional harmattan dust load. North-easterly trade winds carry Saharan and Sahelian dust across central Nigeria from about November to March [7], and harmattan peaks have been recorded at urban sites across West Africa, including a Saharan dust episode in January 2021 that sharply raised $PM_{2.5}$ in Abidjan and Accra [25]. The high $PM_{2.5}/PM_{10}$ ratios of the wet season are a sensor artefact. In the harmattan, however, the plausible ratios (median 0.71) and the high PM_{10} indicate a substantial coarse, mineral component, consistent with both regional dust and local crushing. The second process is surface wetness. Fugitive dust emission from haul roads and stockpiles depends strongly on surface moisture, and road emission estimates are routinely reduced in proportion to the number of rain days [30]. The steep drop in PM between February and March at Q1 and Q3, coinciding with the first rains, is consistent with this control. The third process is atmospheric dilution and activity. The parallel decline of CO and NO_2, which are not removed efficiently by rain, cannot be explained by wet scavenging. It points to deeper convective mixing in the warm, humid months and possibly to lower production in the wet season, when demand for aggregate from road construction is lower [5]. The present data cannot separate these processes because neither meteorology nor production records were collected. Pairing future measurements with wind, humidity and rainfall data and with daily production logs would allow the quarry contribution to be isolated from the regional harmattan background. Diurnally, NO_2 and SO_2 were highest in the morning (0.22 and 0.08 ppm) and lowest at noon (0.14 and 0.04 ppm), and the paired Friedman tests (Figure 3) indicated a consistent ordering of the three times of day for all five pollutants ($p < 0.001$). For PM, however, morning and noon means differed by only 1–2%, and time of day explained less than 0.1% of the variance (Table 3); this ordering, although consistent, is too small to be of practical importance.

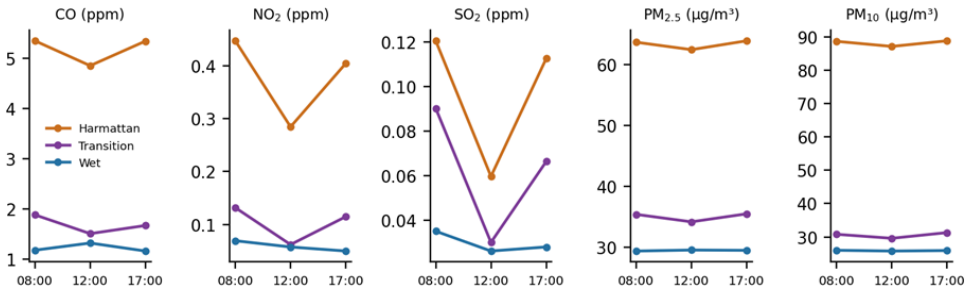

Figure 3. Mean concentrations at 08:00, 12:00 and 17:00 h in each period (Zone A/B Road 2 is excluded from the PM panels)

The diurnal results reinforce this interpretation. NO_2 and SO_2 were highest at 08:00, as the boundary layer is shallow after the stable night and equipment is starting up, and lowest at 12:00, when convective mixing is strongest [8]. Urban sites in Abidjan and Accra show similar morning peaks for $PM_{2.5}$, there driven by rush-hour traffic [25]. In contrast, PM showed no diurnal pattern at monthly resolution. This suggests that dust emission in the quarries, which continues throughout the working day, offsets the dilution that would otherwise lower midday concentrations. For exposure assessment, a single daytime visit therefore represents PM exposure reasonably well, but gas measurements should be taken at several times of day.

3.4 Spatial variation among sampling points

Point-mean concentrations, guideline exceedance and AQI status are listed in Table 4. Figure 4 expresses each point relative to the median of its quarry, so that within-site contrasts can be compared across quarries. Most points fell within ±25% of their site median for PM, which shows that dust was widespread across each quarry rather than confined to one area [5, 6]. Four kinds of departure from this pattern stand out.

Table 4. Six-month mean concentrations at each sampling point, percentage of observations exceeding the WHO 24-h PM2.5 guideline, and percentage classed "Unhealthy" or worse on the AQI (n = 18 observations per point)

Site	Sampling point	CO (ppm)	NO_2 (ppm)	SO_2 (ppm)	$PM_{2.5}$ (µg/m³)	PM_{10} (µg/m³)	$PM_{2.5}$ > WHO (%)	AQI ≥ Unhealthy (%)
Q1	Point 1	1.19	0.147	0.063	45.1	53.7	100	33
Q1	Point 2	1.05	0.171	0.028	38.6	45.7	100	33
Q1	Power house 1	2.28	0.474	0.089	42.3	52.8	100	33
Q1	Power house 2	2.00	0.401	0.109	40.9	50.8	100	33
Q1	Quarry gate	1.30	0.107	0.033	36.0	47.5	89	17
Q1	Outside quarry	0.88	0.118	0.063	31.3	39.9	100	6
Q1	Noble School	0.66	0.077	0.012	23.6	32.5	67	0
Q1	Market	1.74	0.147	0.077	56.8	53.3	100	50
Q2	Point 1	1.31	0.174	0.058	36.7	43.5	100	17
Q2	Point 2	1.28	0.142	0.063	32.9	42.1	100	6
Q2	Power house 1	2.56	0.348	0.075	43.3	47.5	100	17
Q2	Power house 2	2.52	0.417	0.088	44.4	48.8	100	17
Q2	Quarry gate	1.13	0.139	0.050	34.6	39.5	100	0
Q2	Zone A Road 1	0.89	0.089	0.041	32.6	38.5	100	0
Q2	Zone A/B Road 2	2.47	0.339	0.134	327.4	373.8	100	67
Q2	Outside quarry	1.31	0.125	0.039	34.2	43.4	100	0
Q3	Point 1	1.31	0.061	0.039	49.5	51.4	100	33
Q3	Power house 1	2.24	0.122	0.083	47.3	51.6	100	33
Q3	Power house 2	2.12	0.107	0.056	48.0	51.5	100	33
Q3	Quarry gate	2.05	0.072	0.056	47.6	48.4	100	33
Q3	Outside quarry	1.58	0.041	0.042	39.4	41.5	100	33
Q3	Market	25.50	0.144	0.096	89.5	88.9	100	100

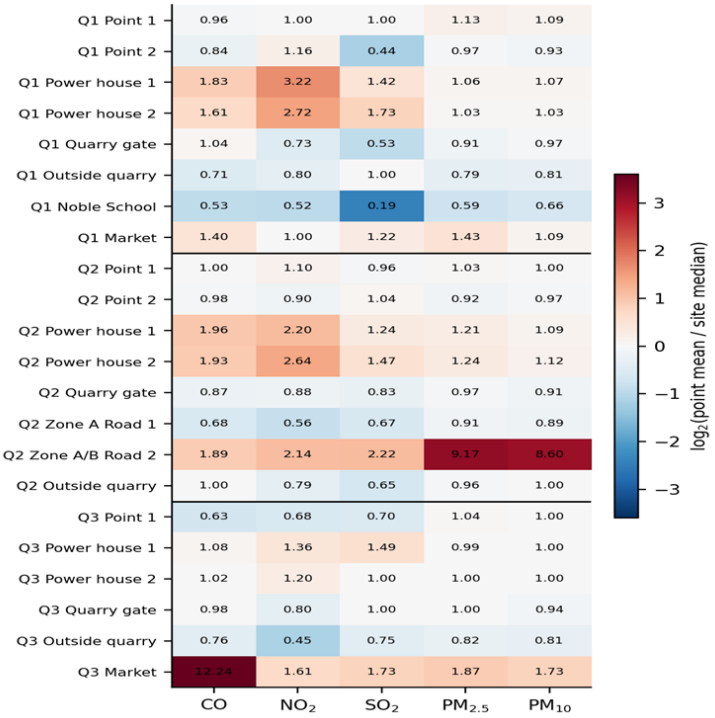

Figure 4. Ratio of each sampling point's mean concentration to the median of the point means at the same quarry (values in cells; colour on a $\log_2$ scale: red above the site median, blue below). Horizontal lines separate Q1, Q2 and Q3

First, the diesel power houses were combustion hotspots at all three quarries. Compared with the other work points (Points 1–2) at the same site, month and time, power houses had higher CO (mean 2.29 vs 1.24 ppm), NO_2 (0.31 vs 0.13 ppm) and SO_2 (0.083 vs 0.048 ppm) (Wilcoxon $p < 0.001$, n = 54 pairs). PM did not differ significantly ($PM_{2.5}$ 44.4 vs 42.0 µg/m³, $p = 0.12$; PM_{10} 50.5 vs 47.9 µg/m³, $p = 0.10$). The contrast was strongest at Q1 and Q2, where NO_2 at the power houses was 2.2–3.2 times the site median (Figure 4). Generators that run throughout the working day are therefore the main source of combustion gases inside the quarries, while dust is generated across the whole working area. Repeating the comparison on point means (six power houses versus five work points) confirmed higher CO (Mann–Whitney $p = 0.008$) and SO_2 ($p = 0.035$) at the power houses. NO_2 was markedly higher at the Q1 and Q2 power houses but not at Q3 (Table 4), so on this basis the NO_2 difference was not significant across all three quarries ($p = 0.25$). These results identify the first of three distinct source signatures, combustion at the power houses. The power houses were enriched in CO, NO_2 and SO_2 but not in PM relative to the other work points, and they lay at the combustion end of PC2 (Section 3.6). This combination is characteristic of diesel generators, which emit nitrogen oxides and CO in proportion to load. The PM they emit is small relative to the crushing dust that surrounds them. The interpolated maps agree with the point statistics: at Q1 and Q2 the NO_2 and CO maxima coincide in the same sector of the quarry. Ayegba et al. [5] likewise found combustion gases concentrated where vehicles and equipment operate, not at the crushing point. A practical consequence is that generator placement and maintenance can reduce worker exposure to combustion gases without affecting dust control, and vice versa. The power-house concentrations can also be placed in context. Diesel generators in Nigeria have been measured at 1 m from the exhaust with CO of 19–198 ppm and $PM_{2.5}$ of 221–492 µg/m³ [31]. The power-house means recorded here (CO about 2–2.6 ppm, NO_2 0.31 ppm) are one to two orders of magnitude lower, as expected at working distances where generator exhaust has mixed with ambient air. They remain clearly above the levels at other work points, which confirms the generators as the main fixed combustion source inside the quarries. Off-grid generators are a large and recognised source of air pollutants in Nigeria [32], and our results show that this applies to industrial sites such as quarries as well as to homes and businesses. Second, Zone A/B Road 2 at Q2 was an extreme but episodic dust hotspot. $PM_{2.5}$ there averaged 144–155 µg/m³ in January–February and 809–816 µg/m³ in March–April

(PM_{10} 898–904 µg/m³), about 23 times the median of the Q2 point means (35.7 µg/m³; the six-month mean of 327 µg/m³ was about nine times it), before falling below 25 µg/m³ in May–June. The March–April values coincide with the end of the dry season, before rains bind the unpaved surface, and are typical of truck-generated dust on dry haul roads. Zone A Road 1 at the same quarry stayed close to or below the site median, which shows how strongly road dust depends on traffic and surface condition at each road. This illustrates the second source signature, dust from haul roads. The extreme PM at Zone A/B Road 2 in March–April, and its collapse once the rains began, fit the well-established dominance of unpaved haul roads in fugitive dust emissions at surface mines. Emission inventories for open-pit mining have identified transport on unpaved roads as the largest single source of total suspended particulates and PM_{10}, and water spraying can reduce total mine emissions by up to about 72% [33]. Dust emission from unpaved roads scales with silt content, vehicle weight and speed, and falls with surface moisture [30]. The contrast between the two Q2 roads (Road 1 near the site median, Road 2 up to about 23 times it) suggests that traffic load and surface condition, rather than proximity to the pit, determine which roads become hotspots. Targeting the busiest roads with watering or chemical suppressants during February–April is therefore likely to be the most cost-effective single measure available at these quarries [6]. Third, the market at Q3 was a CO hotspot, averaging 25.5 ppm (15–36 ppm), 12 times the Q3 median, with $PM_{2.5}$ (89.5 µg/m³) and PM_{10} (88.9 µg/m³) also the highest at that quarry. The market at Q1 was likewise above its site median for $PM_{2.5}$ (1.43 times). Sources unrelated to quarrying therefore contribute substantially at some of the sampled locations, and attributing their pollution to quarrying would need source-specific evidence. This is the third source signature: mixed urban combustion. The Q3 market combined very high CO (mean 25.5 ppm) with modest NO_2, which points to inefficient, low-temperature combustion such as petrol generators, two-stroke motorcycles, idling vehicles and charcoal or wood cooking, rather than to diesel machinery. Its PM was also the highest at Q3. Within-city differences between traffic or source-affected sites and background sites can exceed differences between cities [25], and our results show that the same applies at the scale of a single quarry and its surroundings. Fourth, the lowest values occurred at Noble School (Q1) and at the points recorded as "Outside quarry". Noble School had 34–81% lower concentrations than the Q1 median for all five pollutants, yet its $PM_{2.5}$ still exceeded the WHO 24-h guideline in 67% of observations. The "Outside quarry" points were 0–55% below their site medians.

3.5 Spatial distribution maps

The interpolated surfaces (Figures 5–7) display these point contrasts as within-quarry patterns [13]. At Q1 (Figure 5), all five pollutants increased toward the western side of the mapped area. NO_2 and CO peaked in the north-west and west (above 0.5 ppm and about 2.9 ppm), SO_2 in the south-west (about 0.19 ppm), and $PM_{2.5}$ and PM_{10} formed a steep hotspot along the western edge. Concentrations decreased toward the east, with a low-SO_2 pocket in the north-central area. The coincidence of the NO_2, CO and SO_2 maxima suggests that the western sector contains the main combustion sources, as generators and engines emit these gases together [31, 32].

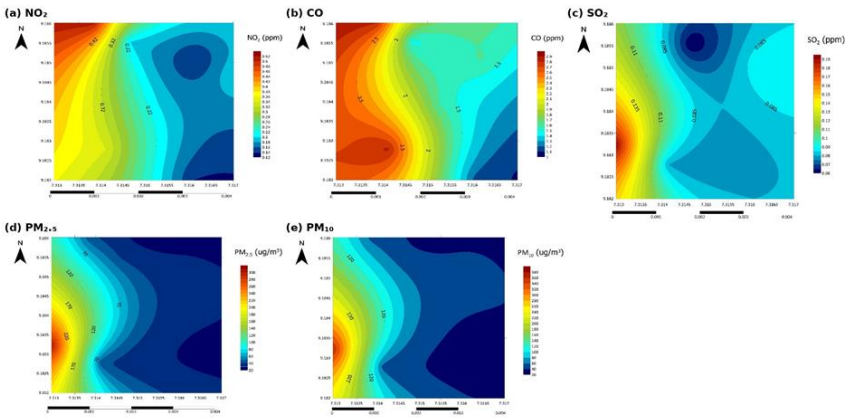

Figure 5. Interpolated spatial distribution of six-month mean (a) NO_2, (b) CO, (c) SO_2, (d) $PM_{2.5}$ and (e) PM_{10} at Q1 (Dutse)

At Q2 (Figure 6), NO_2 (0.08–0.44 ppm) and CO (about 0.5–2.5 ppm) shared a hotspot in the south-west, consistent with a common combustion source [31], and decreased eastward. SO_2 was highest in the north-west (about 0.11 ppm) and lowest in the south-east (about 0.05 ppm). $PM_{2.5}$ peaked in the north-central area (58–60 µg/m³) and PM_{10} in the central and south-western areas (above 55 µg/m³). Both decreased toward the south-east ($PM_{2.5}$ about 34 µg/m³; PM_{10} 38–44.4 µg/m³), which is the main area of dilution. The PM surfaces do not reproduce the Zone A/B Road 2 extremes. Because IDW is an exact interpolator that reproduces the value at every data point [13, 34], this suggests that the road lies at or beyond the mapped area or was excluded from the interpolation.

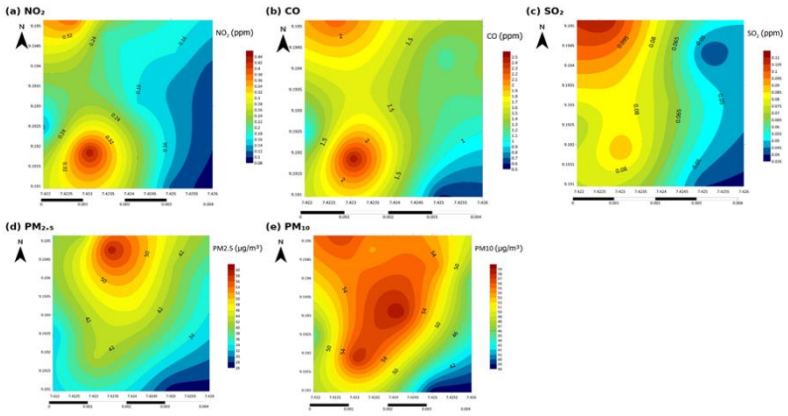

Figure 6. Interpolated spatial distribution of six-month mean (a) NO_2, (b) CO, (c) SO_2, (d) $PM_{2.5}$ and (e) PM_{10} at Q2 (Dutse)

At Q3 (Figure 7), all five pollutants increased toward the south of the mapped area (about 9.181° N). In the south, CO reached above 20 ppm, $PM_{2.5}$ and PM_{10} 80–94 µg/m³, NO_2 0.13–0.16 ppm and SO_2 0.10–0.11 ppm. Concentrations declined toward the north and north-east (CO about 1 ppm, PM about 40–50 µg/m³). The size of the southern CO maximum matches only the market point (Table 4), so the dominant Q3 hotspot reflects market-related combustion, such as small generators, vehicles and cooking fuels, rather than quarry operations [25, 31]. This illustrates why the maps must be read alongside the labels of the points that support them.

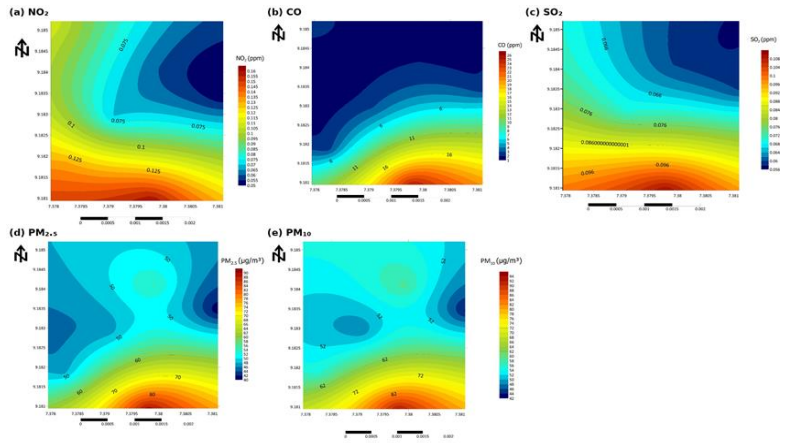

Figure 7. Interpolated spatial distribution of six-month mean (a) NO_2, (b) CO, (c) SO_2, (d) $PM_{2.5}$ and (e) PM_{10} at Q3 (Mpape). Axes in decimal degrees

Two cautions apply to the maps. First, the southern hotspot at Q3 (Figure 7) is produced by the market point, so the maps alone would wrongly suggest a quarry source there. Interpolated surfaces built from a few points of very different character can mislead unless they are read together with point labels and source information. Second, each surface is interpolated from only six to eight points, so values between points and beyond the outermost points are uncertain [34]. The steep western gradients at Q1, which extend beyond the measured range, illustrate the risk of extrapolation at the edges of a

sparse network. The maps are therefore best treated as visual summaries of the point data rather than as independent evidence of dispersion. They also show six-month means, which hide the strong seasonal changes described in Section 3.3. Seasonal maps and denser sampling grids would locate the hotspots more precisely.

3.6 Hotspot typology from multivariate analysis

All five pollutants were positively correlated [18] (Spearman $\rho = 0.39–0.94$, $p < 0.001$). The strongest pairs were $PM_{2.5}$–PM_{10} (0.94), CO–PM_{10} (0.79) and CO–$PM_{2.5}$ (0.77). In the PCA of the 396 observations, PC1 (64.0% of variance) loaded strongly on all pollutants (0.65–0.91) and represents the overall pollution level [19]. Its mean score shifted from the most polluted end in the harmattan to the cleanest in the wet season (Figure 8b), confirming that season dominated. PC2 (16.8%) contrasted PM (loadings +0.36 to +0.41) with NO_2 and SO_2 (−0.47 and −0.57), giving an axis from dust to combustion, in the way PCA is used to separate source types in receptor modelling [35]. On this axis Zone A/B Road 2 had the highest mean score (+0.97) and the power houses the lowest (−0.36 to −0.45).

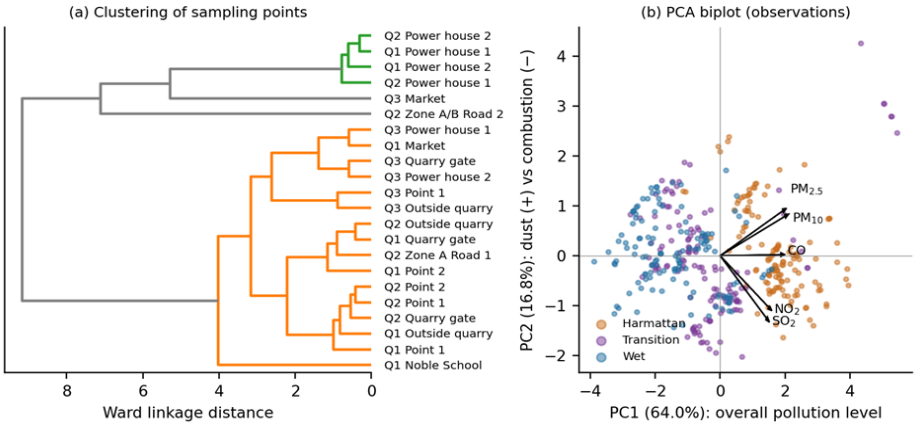

Figure 8. (a) Ward hierarchical clustering of the 22 sampling points on standardised log mean concentrations of the five pollutants. (b) PCA biplot of all observations coloured by period; arrows show loadings (scaled)

Ward clustering (Eq. 4) of the point profiles (Figure 8a) gave the same typology without any prior grouping [20]. Sixteen points formed a general cluster: the work points, gates, "Outside quarry" points, Zone A Road 1, Noble School and the Q1 market. Three hotspot clusters separated from it. The first contained the four power houses of Q1 and Q2, a combustion type [31, 32]. The second was the Q3 market, a CO-dominated combustion type unrelated to quarrying. The third was Zone A/B Road 2, a dust type [30, 33]. The Q3 power houses grouped with the general cluster because CO and PM levels at that quarry were raised throughout. The typology indicates that controls should be targeted by source type rather than applied uniformly: power supply and generator siting for combustion hotspots, and road and surface treatment for dust hotspots. Taken together, the hierarchical clustering and the PCA show that a few distinct hotspots account for much of the spatial variance, while most points share a common, seasonally driven background. This structure has two implications for monitoring design. Fixed networks around quarries should include at least one point at each hotspot type (generator area, main haul road and any nearby combustion-intensive site such as a market), because averages over many general points will hide them. Distances from each point to the working face, together with wind direction, should be recorded so that the decline of concentrations with distance from the source can be quantified.

3.7 Air quality index and health significance

No observation fell in the "Good" AQI category (Eqs. 1-2), mainly because the lowest $PM_{2.5}$ reading (10.5 µg/m³) exceeded the upper limit of that category (9.0 µg/m³) [12]. Across all observations, 46.5% were "Moderate", 26.5% "Unhealthy for Sensitive Groups", 19.7% "Unhealthy", 4.8% "Very Unhealthy" and 2.5% "Hazardous" (Figure 9). $PM_{2.5}$ was the dominant pollutant in 95% of observations,

and CO in the remainder, all at the Q3 market. The share classed "Unhealthy" or worse fell from 65% in the harmattan to 9% in the transition period and 7% in the wet season. At individual points this share ranged from 0% (Noble School, Q2 "Outside quarry", Q2 gate and Zone A Road 1) to 67% at Zone A/B Road 2 and 100% at the Q3 market (Table 4). Fine-particle levels above the WHO guideline have likewise been reported across all monitored sites in Akure [26] and at granite quarries elsewhere in Abuja [5].

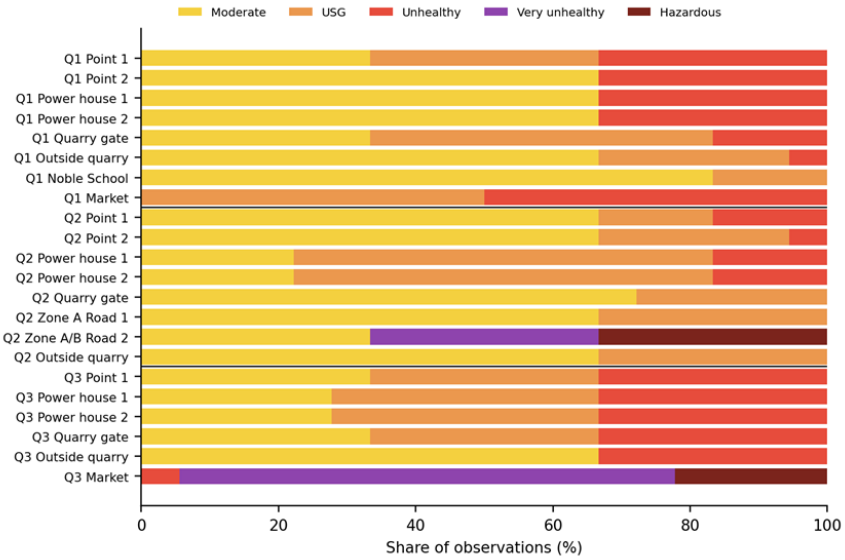

Figure 9. Distribution of AQI categories (U.S. EPA [12]; based on $PM_{2.5}$, PM_{10} and CO) at each sampling point, January–June 2025. USG = Unhealthy for Sensitive Groups

The health significance of these concentrations is dominated by $PM_{2.5}$. It exceeded the WHO 24-h guideline in 98% of observations and drove the AQI in 95%. Meta-analyses underlying the WHO [1] guidelines estimate that each 10 µg/m³ increase in short-term $PM_{2.5}$ raises daily all-cause mortality by about 0.65% [22]. Each 10 µg/m³ increase in long-term exposure raises all-cause mortality by about 8% [23]. Applied illustratively to our data (Eqs. 5-7), the harmattan mean (67 µg/m³) corresponds to a short-term mortality risk about 3.4% higher than at the 24-h guideline level. If the overall median (37 µg/m³) were representative of year-round exposure, the long-term relative risk compared with the WHO annual guideline (5 µg/m³) would be about 1.28. The equivalent figure for the wet-season median (27 µg/m³) is about 1.18. These figures imply that roughly 15–22% of all-cause mortality among people exposed at these levels could be attributable to $PM_{2.5}$. They are indicative only. The measurements cover six daytime months rather than a full year, and spot readings are not personal exposures. The concentration–response functions also come mainly from urban populations exposed to combustion-dominated PM, whereas quarry PM is dominated by mineral dust. They nevertheless show that the levels measured here are of real public-health concern and not merely above a regulatory threshold. For quarry workers, two additional hazards compound PM exposure. Granite is rich in quartz, and respirable crystalline silica in crusher dust causes silicosis and is classified as a human carcinogen [2]. Silica was not measured here, but the high PM levels at the work points make it the priority for occupational monitoring. Workers at the power houses are also exposed to diesel exhaust, which is carcinogenic to humans [36]. Their NO_2 readings, at about 0.31 ppm on average, are roughly three times the WHO 1-h guideline, although this comparison is indicative given the 0.1 ppm sensor resolution. For people at the market and school points, the results show that exposure arises from a combination of quarry and urban sources. Reducing quarry emissions would lower but not remove their risk, and attributing harm to quarrying specifically would require source apportionment using PM elemental composition.

3.8 Reliability of the portable-sensor data

Because $PM_{2.5}$ is a fraction of PM_{10}, the ratio r_{PM} cannot exceed 1. However, the ratio exceeded 1 in 57% of observations (Figure 10). The proportion rose from 3% in the harmattan to 75% in the

transition period and 94% in the wet season, when the median ratio was 1.13. Harmattan ratios were mostly 0.6–0.8 (median 0.71), which is plausible for dust-dominated air. This strong seasonal dependence points to a humidity-related artefact in the optical particle sensor. Hygroscopic growth and size misclassification at high relative humidity are known to bias low-cost optical sensors, and the size channels can respond differently [37, 38]. Transition and wet-season PM values, and especially the $PM_{2.5}/PM_{10}$ partition, should therefore be treated as indicative. Together with the 0.1 ppm resolution of the NO_2 and SO_2 sensors, this means that absolute values and guideline exceedances need confirmation by co-location with reference or gravimetric samplers [27, 28]. The main spatial and seasonal conclusions rest on large relative differences and are robust to these biases.

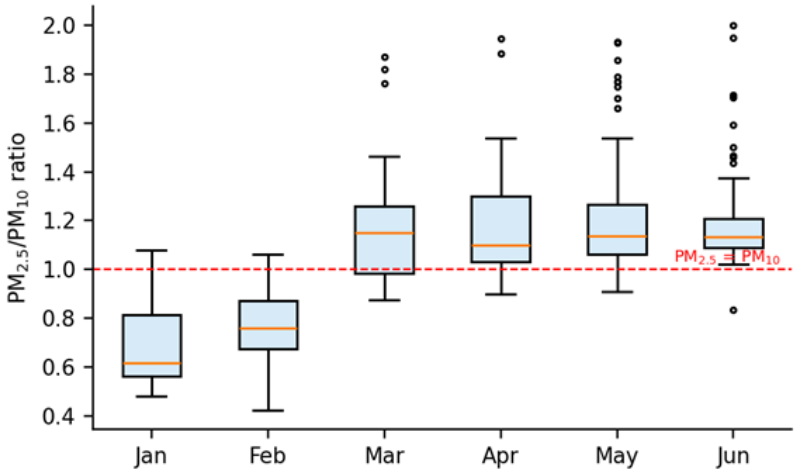

Figure 10. Monthly distribution of the $PM_{2.5}/PM_{10}$ ratio. Values above 1 (dashed line) are physically impossible and indicate sensor bias

Portable and low-cost monitors are increasingly used in Africa, where reference stations are scarce [27, 28]. The present dataset illustrates both their value and their limits. They resolved large relative differences between seasons, points and source types consistently enough to support the conclusions above. However, the $PM_{2.5}/PM_{10}$ ratios above 1 in humid months and the 0.1 ppm resolution of the NO_2 and SO_2 sensors show that uncorrected readings cannot be used for compliance assessment. Hygroscopic growth at high humidity is known to inflate optical PM readings and distort the size distribution they report [37]. Field calibration against reference monitors, as practised in Abidjan and Accra [25], substantially improves accuracy. Studies of quarry air in Nigeria, including this one, should therefore report instrument models, resolution, calibration and relative humidity routinely. Where possible, they should co-locate at least one sensor with a gravimetric or reference instrument for part of the campaign.

3.9 Implications for management

The results point to source-specific measures rather than a uniform approach. Haul-road dust is the largest controllable source and is best addressed by watering or chemical suppression, speed limits and paving of the busiest sections [30, 33], timed for February–April when emissions peak. Generator emissions are best addressed by relocating or venting generators away from work areas, maintaining them regularly and moving progressively to grid or cleaner power [31, 32]. Crusher dust calls for enclosure and water sprays [6]. Because the harmattan raises background PM regardless of quarry practice, intensified controls and mandatory use of certified respirators (at least FFP2/N95) during January–April would give the greatest protection per unit of effort. Personal protective equipment is already the most widely used safety measure on construction sites in Abuja [39], which suggests that respirator programmes would be practicable locally. For regulators, national and WHO particulate standards are defined for 24-h averages [1]. Compliance monitoring around quarries therefore needs continuous or at least full-day sampling with calibrated instruments, and should include nearby sensitive locations such as schools and markets.

4 CONCLUSIONS

Monitoring of five pollutants at 22 sampling points in three granite quarries in Abuja from January to June 2025 led to the following conclusions. (1) $PM_{2.5}$ exceeded the WHO 24-h guideline in 98% of observations, and PM_{10} in all January–February observations. AQI categories were never "Good", and 65% of harmattan observations were "Unhealthy" or worse. (2) Season was the largest source of variability for most pollutants (15–50% of variance), followed by sampling point (15–35%). Time of day mattered only for NO_2 and SO_2, which peaked in the morning. Mean concentrations fell by 57–84% from the harmattan to the wet season. (3) Diesel power houses were consistent combustion hotspots, with CO 1.8 times, NO_2 2.4 times and SO_2 1.7 times the levels at other work points (NO_2 mainly at the two Dutse quarries), whereas PM was similar across work points. A haul road at Q2 produced episodic hazardous PM above 800 µg/m³, and the Q3 market showed a CO hotspot (mean 25.5 ppm) unrelated to quarry machinery. (4) Interpolated maps, built from six to eight points per quarry, indicated spatial gradients within each quarry: towards the west at Q1, the south-west (gases) and north-central (PM) at Q2, and the south at Q3. Clustering and PCA separated combustion-type and dust-type hotspots from a general background, which supports source-specific controls. (5) The portable sensors resolved relative spatial and seasonal patterns, but humidity bias in PM size fractions and coarse gas resolution limit their use for compliance assessment. Future work should co-locate sensors with reference samplers, record meteorology, monitor over a full year with denser spatial coverage, and determine PM composition, including respirable crystalline silica and metals.

REFERENCES

1. World Health Organization (2021). Global Air Quality Guidelines: Particulate Matter (PM2.5 and PM10), Ozone, Nitrogen Dioxide, Sulfur Dioxide and Carbon Monoxide. *Geneva, Switzerland: WHO, 2021*, 273p.
2. International Agency for Research on Cancer (2012). Silica dust, crystalline, in the form of quartz or cristobalite. *Arsenic, Metals, Fibres, and Dusts, IARC Monographs on the Evaluation of Carcinogenic Risks to Humans, vol. 100C. Lyon, France: IARC*, pp. 355-405.
3. Enoh, E.A., Ogwo, P.A. and Ubuoh, E.A. (2023). Impact of particulate matter as an air quality pollutant released from quarry activities in Akamkpa, Cross River State, Nigeria. *African Journal of Environment and Natural Science Research*, vol. 6, no. 3, pp. 1-25.
4. Omeiza, L.M., Sangari, D.U. and Ogah, A.T. (2022). Effects of quarrying on air quality in Mpape, Bwari Area Council, FCT Abuja, Nigeria. *International Journal of Environmental Research and Earth Science*, vol. 24, no. 4, pp. 1-10.
5. Ayegba, K., Tyovenda, A.A. and Audu, M.O. (2025). Environmental monitoring of air pollutants in the vicinity of major granite mining and processing sites in Abuja, Nigeria. *Polish Journal of Natural Sciences*, vol. 40, no. 4, pp. 215-227.
6. Patra, A.K., Gautam, S. and Kumar, P. (2016). Emissions and human health impacts of particulate matter from surface mining operations – A review. *Environmental Technology & Innovation*, vol. 5, pp. 233-249.
7. Prospero, J.M., Ginoux, P., Torres, O., Nicholson, S.E. and Gill, T.E. (2002). Environmental characterization of global sources of atmospheric soil dust identified with the NIMBUS 7 Total Ozone Mapping Spectrometer (TOMS) absorbing aerosol product. *Reviews of Geophysics*, vol. 40, no. 1, art. no. 1002, pp. 2-31.
8. Stull, R.B. (1988). An Introduction to Boundary Layer Meteorology. Dordrecht, The Netherlands: *Kluwer Academic Publishers*, pp. 1-27.
9. ASTM International (2019). Standard Practice for Planning the Sampling of the Ambient Atmosphere, ASTM D1357-95 (Reapproved 2019). *West Conshohocken, PA, USA: ASTM International*, pp. 1-4.

10. Seinfeld, J.H. and Pandis, S.N. (2016). Atmospheric Chemistry and Physics: From Air Pollution to Climate Change, 3rd ed. *Hoboken, NJ, USA: Wiley*, ch. 1, pp. 1-15.

11. George, C. (2026). Risk assessment of air pollutants and heavy metals in quarry producing sites in Federal Capital Territory, Abuja, Nigeria. *Ph.D. dissertation, Dept. of Chemistry, Nasarawa State University, Keffi, Nigeria*.

12. U.S. Environmental Protection Agency (2024). Technical Assistance Document for the Reporting of Daily Air Quality – the Air Quality Index (AQI), EPA-454/B-24-002. *Research Triangle Park, NC, USA: Office of Air Quality Planning and Standards*, May 2024.

13. Shepard, D. (1968). A two-dimensional interpolation function for irregularly-spaced data. *Proceedings of the 1968 23rd ACM National Conference, New York, NY, USA: ACM*, pp. 517-524.

14. Montgomery, D.C. (2017). Design and Analysis of Experiments, 9th ed. *Hoboken, NJ, USA: Wiley*, ch. 3 and 5, pp. 1-20.

15. Kruskal, W.H. and Wallis, W.A. (1952). Use of ranks in one-criterion variance analysis. *Journal of the American Statistical Association*, vol. 47, no. 260, pp. 583-621.

16. Wilcoxon, F. (1945). Individual comparisons by ranking methods. *Biometrics Bulletin*, vol. 1, no. 6, pp. 80-83.

17. Friedman, M. (1937). The use of ranks to avoid the assumption of normality implicit in the analysis of variance. *Journal of the American Statistical Association*, vol. 32, no. 200, pp. 675-701.

18. Spearman, C. (1904). The proof and measurement of association between two things. *American Journal of Psychology*, vol. 15, no. 1, pp. 72-101.

19. Jolliffe, I.T. (2002). Principal Component Analysis, 2nd ed. *New York, NY, USA: Springer*, ch. 1-3.

20. Ward, J.H. (1963). Hierarchical grouping to optimize an objective function. *Journal of the American Statistical Association*, vol. 58, no. 301, pp. 236-244.

21. Zar, J.H. (2010). Biostatistical Analysis, 5th ed. *Upper Saddle River, NJ, USA: Pearson Prentice Hall*, ch. 8 and 10, pp. 1-10.

22. Orellano, P., Reynoso, J., Quaranta, N., Bardach, A. and Ciapponi, A. (2020). Short-term exposure to particulate matter (PM10 and PM2.5), nitrogen dioxide (NO2), and ozone (O3) and all-cause and cause-specific mortality: Systematic review and meta-analysis. *Environment International*, vol. 142, art. no. 105876, 2020.

23. Chen, J. and Hoek, G. (2020). Long-term exposure to PM and all-cause and cause-specific mortality: A systematic review and meta-analysis. *Environment International*, vol. 143, art. no. 105974, 2020.

24. Rockhill, B., Newman, B. and Weinberg, C. (1998). Use and misuse of population attributable fractions. *American Journal of Public Health*, vol. 88, no. 1, pp. 15-19.

25. Bahino, J., Giordano, M., Beekmann, M., Yoboué, V., Ochou, A., Galy-Lacaux, C., Liousse, C., Hughes, A., Nimo, J., Lemmouchi, F., Cuesta, J., Amegah, A.K. and Subramanian, R. (2024). Temporal variability and regional influences of PM2.5 in the West African cities of Abidjan (Côte d'Ivoire) and Accra (Ghana). *Environmental Science: Atmospheres*, vol. 4, no. 4, pp. 468-487.

26. Saetae, S., Abulude, F.O., Ndamitso, M.M., Akinnusotu, A., Oluwagbayide, S.D., Matsumi, Y., Kanegae, K., Kawamoto, K. and Nakayama, T. (2024). Multi-year continuous observations of ambient PM2.5 at six sites in Akure, southwestern Nigeria. *Atmosphere*, vol. 15, no. 7, art. no. 867.

27. Kumar, P., Morawska, L., Martani, C., Biskos, G., Neophytou, M., Di Sabatino, S., Bell, M., Norford, L. and Britter, R. (2015). The rise of low-cost sensing for managing air pollution in cities. *Environment International*, vol. 75, pp. 199-205.

28. Morawska, L., Thai, P.K., Liu, X., Asumadu-Sakyi, A., Ayoko, G., Bartonova, A., Bedini, A., Chai, F., Christensen, B., Dunbabin, M., Gao, J., Hagler, G.S.W., Jayaratne, R., Kumar, P., Lau, A.K.H., Louie, P.K.K., Mazaheri, M., Ning, Z., Motta, N., Mullins, B., Rahman, M.M., Ristovski, Z., Shafiei, M., Tjondronegoro, D., Westerdahl, D. and Williams, R. (2018). Applications of low-cost sensing technologies for air quality monitoring and exposure assessment: How far have they gone. *Environment International*, vol. 116, pp. 286-299.

29. Shittu, A.I., Pope, R.J., Pringle, K.J., Arnold, S.R., Graham, A.M., Sideeq, H.O., Ana, G.R.E.E. and McQuaid, J.B. (2025). Quantifying residential particulate pollution and human exposure in Ibadan, Nigeria, using low-cost sensors. *Aerosol and Air Quality Research*, vol. 25, art. no. 44, 2025.

30. U.S. Environmental Protection Agency (2006). Section 13.2.2: Unpaved roads. *Compilation of Air Pollutant Emission Factors (AP-42), vol. I, 5th ed. Research Triangle Park, NC, USA: U.S. EPA*, pp. 13.2.2-1–13.2.2-20.

31. Giwa, S.O., Nwaokocha, C.N. and Adeyemi, H.O. (2019). Noise and emission characterization of off-grid diesel-powered generators in Nigeria. *Management of Environmental Quality*, vol. 30, no. 4, pp. 783-802.

32. Adeniran, J.A., Yusuf, R.O., Amole, M.O., Jimoda, L.A. and Sonibare, J.A. (2017). Air quality impact of diesel back-up generators (BUGs) in Nigeria's mobile telecommunication base transceiver stations (BTS). *Management of Environmental Quality*, vol. 28, no. 5, pp. 723-744.

33. Huertas, J.I., Camacho, D.A. and Huertas, M.E. (2012). Standardized emissions inventory methodology for open-pit mining areas. *Environmental Science and Pollution Research*, vol. 19, no. 7, pp. 2784-2794.

34. Oliver, M.A. and Webster, R. (1990). Kriging: A method of interpolation for geographical information systems. *International Journal of Geographical Information Systems*, vol. 4, no. 3, pp. 313-332.

35. Thurston, G.D. and Spengler, J.D. (1985). A quantitative assessment of source contributions to inhalable particulate matter pollution in metropolitan Boston. *Atmospheric Environment*, vol. 19, no. 1, pp. 9-25.

36. Benbrahim-Tallaa, L., Baan, R.A., Grosse, Y., Lauby-Secretan, B., El Ghissassi, F., Bouvard, V., Guha, N., Loomis, D. and Straif, K. (2012). Carcinogenicity of diesel-engine and gasoline-engine exhausts and some nitroarenes. *The Lancet Oncology*, vol. 13, no. 7, pp. 663-664.

37. Jayaratne, R., Liu, X., Thai, P., Dunbabin, M. and Morawska, L. (2018). The influence of humidity on the performance of a low-cost air particle mass sensor and the effect of atmospheric fog. *Atmospheric Measurement Techniques*, vol. 11, no. 8, pp. 4883-4890.

38. Castell, N., Dauge, F.R., Schneider, P., Vogt, M., Lerner, U., Fishbain, B., Broday, D. and Bartonova, A. (2017). Can commercial low-cost sensor platforms contribute to air quality monitoring and exposure estimates. *Environment International*, vol. 99, pp. 293-302.

39. Jimoh, R.A., Oyewobi, L.O., Isa, R.B. and Momoh, A.S. (2017). Level of adherence to safety measures on construction sites in Abuja, Nigeria. *International Science and Technology Journal of Namibia*, vol. 10, pp. 3-22.